Solvent-dependent dual emission processes in charge-transfer excited states of phenothiazine-triphenyltriazine conformers

Tomohiro Ryu[1], Kiyoshi Miyata[1], Masaki Saigo[1], Yuushi Shimoda[1], Youichi Tsuchiya[2], Hajime Nakanotani[2], Chihaya Adachi[2], Ken Onda[1*]

[1]Department of Chemistry, Faculty of Science, Kyushu University
744 Motooka, Nishi, Fukuoka 819-0395, Japan
[2]Center for Organic Photonics and Electronics Research, Kyushu University
744 Motooka, Nishi, Fukuoka 819-0395, Japan
*e-mail address: konda@chem.kyushu-univ.jp

Abstract

We have investigated the solvent effects on charge-transfer excited states in a donor-acceptor type luminescent material, phenothiazine-triphenyltriazine (PTZ-TRZ), which has characteristic two conformers: quasi-axial and quasi-equatorial conformers. Solvent permittivity dependence of steady-state photoluminescence spectra using mixture solvents of toluene and tetrahydrofuran (THF) indicated that the two conformers have almost the same excited-state dipole moments. Time-resolved photoluminescence and transient absorption spectra in toluene and THF showed a different solvent dependence between the two conformers. From the detailed analysis of these time-resolved spectra, we revealed the solvent-dependent emission processes in the two conformers.

Introduction

Charge-transfer (CT) excited state of an organic molecule is an excited state where a significant charge distribution change occurs within or between molecules upon an electronic transition. Molecules with CT excited states are characterized by spatially separated transition orbitals. Characteristic properties of CT excited states have been utilized for many applications: near-infrared bioimaging which utilizes a large Stokes shift in light emission originating from a CT excited state [1,2], organic photovoltaic devices which utilize intermolecular charge transfer [3,4], and organic light-emitting diodes which utilize characteristic emission from a CT excited state including thermally activated fluorescence (TADF) [5–8].

There are two important properties of CT excited states from an application viewpoint: (1) significant energy stabilization due to solvation and (2) a small energy gap between the lowest singlet excited state (S_1) and the lowest triplet excited state (T_1) due to small overlap integral of frontier molecular orbitals. The former is the phenomenon that energies of CT excited states in a solute molecule are stabilized by reorientation of the surrounding solvent molecules. As the permittivity of the solvent increases, the energy of the CT excited state is lowered, and the emission spectrum is red-shifted [9,10]. The latter is the property that the spatial separation of transition orbitals reduces the exchange interaction because the energy separation between the singlet and triplet states is determined

by the exchange interaction between orbitals. When the energy gap becomes comparable to the thermal energy of room temperature, reverse intersystem crossing (RISC) from T_1 to S_1 occurs and TADF is observed [11–13]. Since the CT excited states have a significant influence on the optical functions of molecules, elucidating the properties and dynamics of CT excited states is of great importance.

Phenothiazine-triphenyltriazine (PTZ-TRZ, inset in Figure 1a), composed of an electron-donor PTZ and an electron-acceptor TRZ, has unique optical properties originating from the CT excited states. PTZ-TRZ shows dual emission (Figure 1a) upon photoexcitation and the photophysical properties of both the emission bands depend on the permittivity of a solvent, implying that the two bands originate from two different CT excited states [14,15]. Quantum chemical calculations predicted that PTZ-TRZ has two stable geometries, quasi-axial conformer (q-ax.) and quasi-equatorial conformer (q-eq.) (Figure 1b), in both the ground and excited states [14,15]. The two emission bands are expected to be assigned to the emissions from these two conformers. Most of dual emission in an organic molecule were attributed to the transitions from a CT excited and a locally excited (LE) states [16–19]; therefore, this dual emission from two CT excited states of two conformers is quite unusual. To date, Tanaka et al. reported that only q-eq. exhibits TADF and q-ax. undergoes a structural relaxation to q-eq.[14] and Chou et al. reported that the time constant of the relaxation is arpprox. 1.8 ps [15] (Figure 1c). Nevertheless, the previous studies carried out only in low-permittivity solvents although solvent dependence of the optical properties of CT excited states are critical to the microscopic understanding of CT excited states.

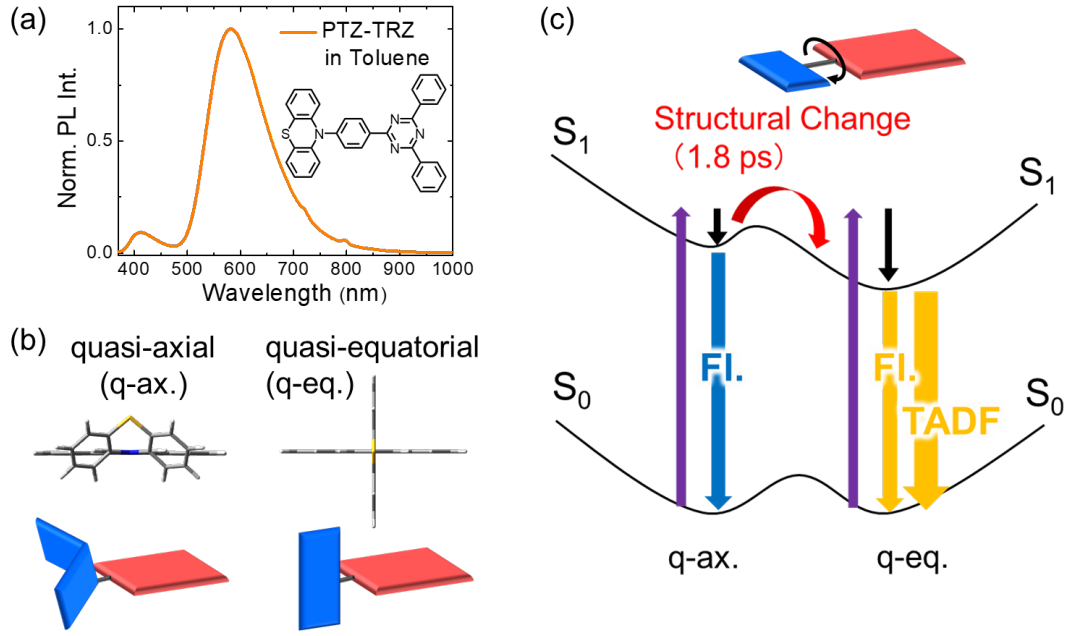

Figure 1. (a) Emission spectrum of PTZ-TRZ in toluene upon 360 nm photoexcitation. Inset: chemical structure of PTZ-TRZ. (b) Geometries of quasi-axial (q-ax.) and quasi-equatorial (q-eq.) conformers. (c) Potential energy curves of PTZ-TRZ predicted from the previous studies.

To understand the mechanism of dual emission in the excited states, it is important to reveal experimentally the properties and dynamics of the CT excited states in the two conformers. In this study, since the solvation of the CT excited states are dependent on the permittivity of the solvent, we used two solvents with different permittivity (ε), toluene (ε = 2.38) and tetrahydrofuran (THF, ε = 7.58), and investigated the properties and dynamics of the CT excited states using spectroscopic measurements. The steady-state photoluminescence (PL) spectra for the two solvents showed different relative emission intensities between the two conformers whereas their absorption spectra are almost the same. By analyzing the photoluminescence spectra in mixture solvents with different ratios between toluene and THF, we found that the dipole moments of the CT excited states of q-ax. and q-eq. are almost identical. The time-resolved PL (TR-PL) spectra in toluene and in THF showed a different behavior: TADF from q-eq. is significantly suppressed in THF whereas the emission from q-ax. showed little change. From the transient absorption (TA) spectra, we found that the time constants of structural change from q-ax. to q-eq. are insensitive to the solvent. Based on these results, we proposed a new energy diagram and emission mechanism in CT excited states of PTZ-TRZ.

Experimental

Steady-state PL spectroscopy

Steady-state PL spectra were measured by a CCD camera (Andor, Newton 920P BEX2-DD) equipped with a polychromator (Andor, Kymera 193i-B2). The light source for optical excitation was a Ti:sapphire regenerative amplifier (Spectra-Physics, Spitfire Ace, pulse duration = 120 fs, repetition rate = 1 kHz, pulse energy = 4 mJ/pulse, central wavelength = 800 nm). The fourth harmonic (360 nm) of the signal light (1440 nm) from an optical parametric amplifier (OPA, Light Conversion, TOPAS) pumped by the regenerative amplifier was used for sample excitation. The concentration of the solutions was 0.1 mM.

TR-PL spectroscopy

TR-PL spectra were measured by a polychromator and a streak camera system (Hamamatsu C4780, time resolution: < 30 ps). The sample excitation pulse was the same as the steady-state PL spectroscopy (360 nm). The polarizations of the excitation and detection lights was set to the magic angle configuration (~54.7°). The concentration of the sample solutions was prepared to be 0.1 mM. All measurements were conducted after one-hour bubbling using N_2 gas.

TA spectroscopy

TA spectra were measured by the pump-probe method [20–22]. For a probe pulse, we generated a white light pulse by focusing the signal light (1200 nm) from another OPA (Light Conversion, TOPAS-Prime) on a sapphire crystal (3 mm thickness). For the pump pulse, we employed one of the

two pulses below accordingly depending on the measurement time range. In the picosecond range, we used the same excitation pulse as the steady-state PL spectroscopy (360 nm). In the nanosecond range, we used the third-harmonic (355 nm) of the output from a Nd:YAG laser (EKSPLA NT242, central wavelength: 1064 nm, pulse duration: 6 ns). The pump pulse fluences at the sample position were 0.34 mJ/cm^2 for picosecond measurements, 0.81 mJ/cm^2 (in toluene) and 1.63 mJ/cm^2 (in THF) for nanosecond measurements. The polarizations of the pump and probe pulses was set to the magic angle configulration (~54.7°). The probe pulse passed through the sample solution was dispersed by a polychromator (JASCO, CT-10, 300 grooves / 500 nm), and the spectra were recorded by a multichannel detection system with a CMOS sensor (UNISOKU, USP-PSMM-NP). The concentration of the sample solutions was prepared to be 0.1 mM. All measurements were conducted with N_2 gas bubbling.

Quantum Chemical Calculations

Quantum chemical calculations were performed using *Gaussian 16* package [23]. The geometries of the ground state (S_0) were optimized based on density functional theory (DFT), and the properties of S_1 and T_1 were calculated using the optimized geometries of the ground state (S_0) based on time-dependent (TD)-DFT. We employed the 6-31G(d,p) basis set and B3LYP functional.

Sample Preparation.

We synthesized PTZ-TRZ according to previous works [14]. We prepared solutions of the purified molecules in toluene and THF purchased from Kanto Chemical Co..

Results and discussion

Figure 2a compares the UV-Vis absorption and steady-state PL spectra of PTZ-TRZ in toluene and THF. The two bands at ~290 nm and 363 nm in the absorption spectra are located at almost the same wavelengths both in toluene and in THF, indicating that the optical transitions from S_0 are independet of solvent or permittivity. In contrast, the PL spectra depend largely on the solvent. The PL spectra in both solutions show dual emission and their bands are located at 422 nm and 576 nm in toluene and at 453 nm and 675 nm in THF. According to the quantum chemical calculations, the emission bands at 453 and 675 nm are assigned to the emissions from q-ax. and q-eq., respectively [14]. Both the emission bands are red-shifted in the higher permittivity solvent (THF), indicating that the excited-state energies of both the conformers are stabilized by the solvation. Thus, both the two excited states showing these emissions are assigned to CT excited states. This result is consistent with the previous reports [14,15].

The intensity ratio of the two emission bands also depends on the solvent, indicating that the excited states in the two conformers are differently affected by the solvent. In order to quantitively

investigate the effect of solvent on the excited states in each conformer, we measured the steady-state PL spectra in the mixed solvents of toluene and THF with varying the mixing ratio. This allows us to continuously change the solvent permittivity between those of toluene (2.38) and THF (7.58) (Figure 2b). The intensities of the emission bands assigned to q-ax. with a peak ranging from 422 nm to 453 nm were almost independent of solvent permittivity. On the other hand, the intensities of the emission bands assigned to q-eq. with a peak ranging from 576 nm to 675 nm decreased significantly with increasing solvent permittivity.

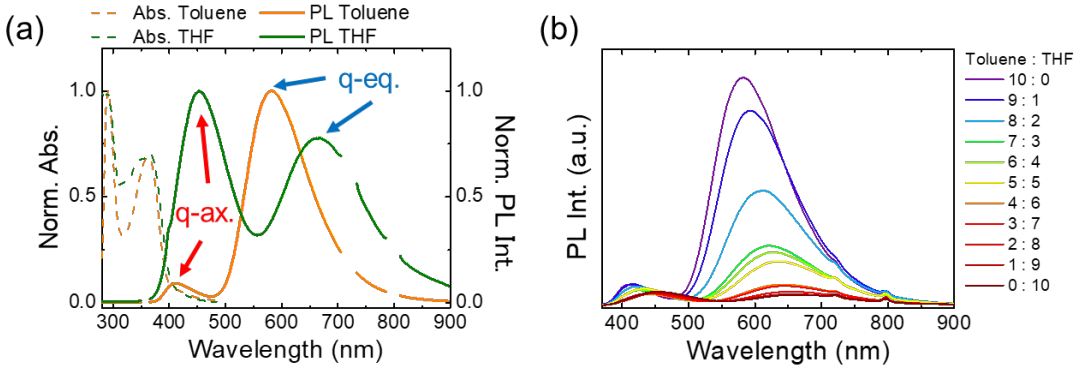

Figure 2. (a) Absorption (dashed lines) and steady-state PL (solid lines) spectra of PTZ-TRZ in toluene and THF. The region 350 - 365 nm, 705 - 733 nm and 785 - 810 nm has been removed because of strong scattered light from the laser. (b) Steady-state PL spectra of mixture solutions of toluene and THF with varying mixing ratios. The concentration of the solutions was 0.1 mM and the excitation wavelength of PL measurements was 360 nm.

It is known that the permittivity dependence of absorption and emission bands are expressed by the Mataga-Lippert equation [24–26],

$$\nu_{\mathrm{Abs.}} - \nu_{\mathrm{Emi.}} = \frac{\left|\mu_{\mathrm{e}} - \mu_{\mathrm{g}}\right|^2}{hca^3}\Delta f \; + \; Constant \tag{1}$$

$$\Delta f = \left(\frac{\varepsilon - 1}{2\varepsilon + 1} - \frac{n^2 - 1}{2n^2 + 1}\right) \tag{2}$$

where h is Planck's constant, c is the speed of light in a vacuum, μ_{e} and μ_{g} are dipole moments of excited- and ground-state, respectively, a is an Onsager cavity radius of solute, ε is a permittivity of solvent, n is a refractive index of solvent. This equation means that the Stokes shift from an absorption band to an emission band is proportional to the square of the difference in dipole moments between excited and ground states and varies on permittivity and refractive index of solvent. This equation allows us to estimate the excited-state dipole moments of the two conformers shown in Figure 2b.

The parameters used for our estimations are summarized in Table 1. The dipole moments of the

ground state (μ_g = 2.95 D for q-ax. and μ_g = 3 .05 D for q-eq.) and the Onsager cavity radii (a = 6.41 Å for q-ax., a = 6.44 Å for q-eq.) were calculated by the quantum chemical calculations. For the values of ε and n, we used the values reported by Loukova *et al*. [27] The values of the permittivity of the mixture solvents $\varepsilon_{\mathrm{mix}}$ were calculated by the following equation [28],

$$\varepsilon_{\mathrm{mix}} = \phi_{\mathrm{toluene}}\varepsilon_{\mathrm{toluene}} + \phi_{\mathrm{THF}}\varepsilon_{\mathrm{THF}} \quad (3)$$

where $\varepsilon_{\mathrm{toluene}}$ and $\varepsilon_{\mathrm{THF}}$ are the permittivity of toluene and THF, respectively. ϕ_{toluene} and ϕ_{THF} are the weight fractions of toluene and THF in the mixture solutions, respectively. Also, the values of the refractive index of the mixture solutions n_{mix} were calculated by the following equation [29],

$$n_{\mathrm{mix}} = \phi_{\mathrm{toluene}}n_{\mathrm{toluene}} + \phi_{\mathrm{THF}}n_{\mathrm{THF}} \quad (4)$$

where n_{toluene} and n_{THF} are the permittivity of toluene and THF, respectively. Figure 3a plots the Stokes shift (cm^{-1}) as a function of the solvent parameter (Δf) for the bands assigned to q-eq. (red dots) and q-ax. (green dots). Both the plots were proportional to Δf, indicating that the Mataga-Lippert equation is well applicable to this system. Thus, the dipole moments of the excited states are reasonably derived from the slopes of these plots. By the linear least squares fit (solid lines in Figure 3a), we determined the excited-state dipole moments of q-eq. and q-ax. to be 20.8 D and 23.2 D, respectively. This result means that the excited states of both the conformers have almost the same dipole moment though their conformations are largely different.

Table 1 . Parameters used for the Mataga-Lippert plot for each mixture solvent. $\nu_{\mathrm{Abs.}} - \nu_{\mathrm{Emi.}}$, ε, and n are the values of Stokes shift, permittivity of solvent, and refractive index of solvent, respectively. The values of Δf were calculated with the value of ε and n in each mixture by the equation (2).

Toluene : THF	$\nu_{\mathrm{Abs.}} - \nu_{\mathrm{Emi.}}$		$\varepsilon_{\mathrm{mix}}$	n_{mix}	Δf
	q-ax.	q-eq.			
10 : 0	3606	100887	2.38[a]	1.496[a]	0.0135
9 : 1	3852	11190	2.90	1.485	0.0567
8 : 2	4226	11625	3.42	1.474	0.0892
7 : 3	4539	11927	3.94	1.464	0.1148
6 : 4	4759	12077	4.46	1.454	0.1356
5 : 5	4920	12287	4.98	1.446	0.1528
4 : 6	5202	12444	5.50	1.437	0.1674
3 : 7	5336	12499	6.02	1.429	0.1800
2 : 8	5621	12698	6.54	1.424	0.1911
1 : 9	5891	12769	7.06	1.414	0.2009
0 : 10	5964	12938	7.58[a]	1.407[a]	0.2094

To rationalize the little difference in the excited-state dipole moments between the two conformers, we performed TD-DFT calculations and calculated natural transition orbital (NTO) [30]. Figure 3b shows the highest occupied NTO (HONTO) and lowest unoccupied NTO (LUNTO) of the lowest singlet excited state, S_1. In both the conformers, the transition orbitals are localized mainly at the PTZ moiety in HONTO and mainly at the TRZ moiety in LUNTO, indicating that both are CT excited states. The excited-state dipole moments for q-ax. and q-eq. were calculated to be 25.0 D and 22.6 D, respectively, which are in good agreement with the experimental values estimated from the Mataga-Lippert plots, 23.2 D and 20.8 D, respectively. Thus, we concluded that the large solvent dependence of emission spectra between the two conformers is not caused by the differences in their dipole moment.

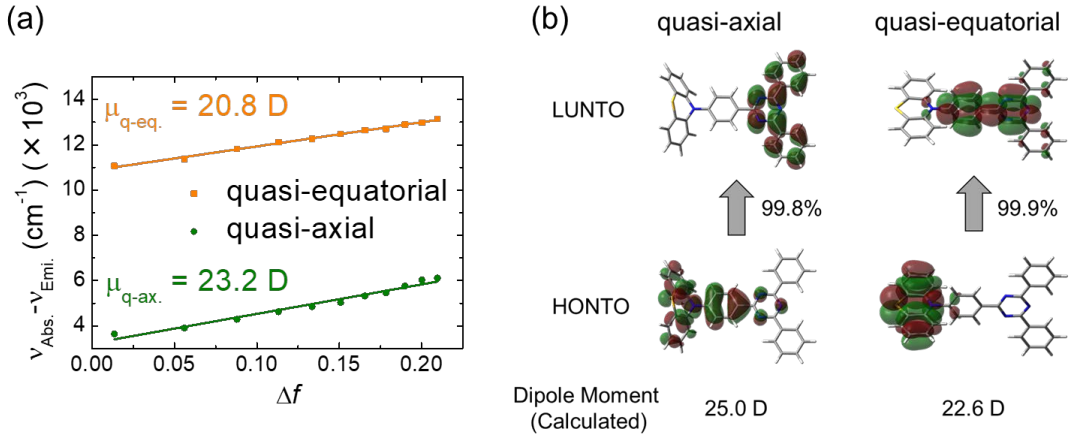

Figure 3. (a) Plots of Stokes shift ($\nu_{\mathrm{Abs.}} - \nu_{\mathrm{Emi.}}$) vs. Δf on the basis of Mataga-Lippert equation (details are described in the text). Orange and green dots represent the data of q-eq. and q-ax., respectively, and their linear lines are obtained by the linear least squares fit. (b) NTOs and calculated dipole moments for S_1 of the two conformers .

To explore the causes of the different solvent dependence of emission spectra between the two conformers, we investigated the dynamical processes in their excited states using time-resolved spectroscopies. Figure 4a compares the TR-PL spectra of the q-ax. band at 0 and 2.5 ns after photoexcitation. Figure 4b compares the spectra of the q-eq. band at 0 and 500 ns in toluene. Figure 4c compares the spectra of the q-ax band at 0 and 2.5 ns in THF. Figures 4d-4f show the decay profiles of TR-PL spectra of the q-eq. band up to 15 ns (d) and 1000 ns (e) and of the q-ax. band up to 10 ns (f) in toluene and in THF.

The decay profiles of the q-eq. band in toluene shown in Figures 4d and 4e clearly shows a double exponential decay with lifetimes of 16 ± 0.1ns and 544 ± 12 ns, respectively. Because the band shape is independent of the delay time as shown in Figure 4b, the shorter and longer lifetime decays are assigned to the lifetimes of prompt fluorescence and TADF, respectively. In THF, the lifetime of

prompt fluorescence becomes much shorter, 0.97 ± 0.01 ns and no TADF is observed. This result indicates that the nonradiative decay from S_1 to S_0 is accelerated in a higher permittivity solvent in q-eq. This is presumably because the solvation by a higher permittivity solvent heavily stabilized the CT excited S_1 state and the smaller energy gap between S_1 and S_0 (Figure 2a) causes efficient nonradiative decay, which is known as the energy gap law [31]. This nonradiative acceleration mechanism also explains the experimental fact that the intensity of steady-state emission decreases with increasing the permittivity of solvent as shown in Figure 2b.

The decay profiles of the q-ax. band shown in Figure 4f also show a double exponential decay both in toluene and in THF but the peak position of the band is red-shifted at the longer delay time as shown in Figures 4a, 4c. Because the shorter lifetime is estimated to be shorter than the instrument response function (IRF ~ 1 ns), the faster process in the excited state occurs in less than 1 ns. Since the structural change from q-ax. to q-eq. occurs in less than 1 ns [15], the shorter lifetime is at least partially attributed to this structural change. In contrast to the q-eq. band, the longer lifetime is not

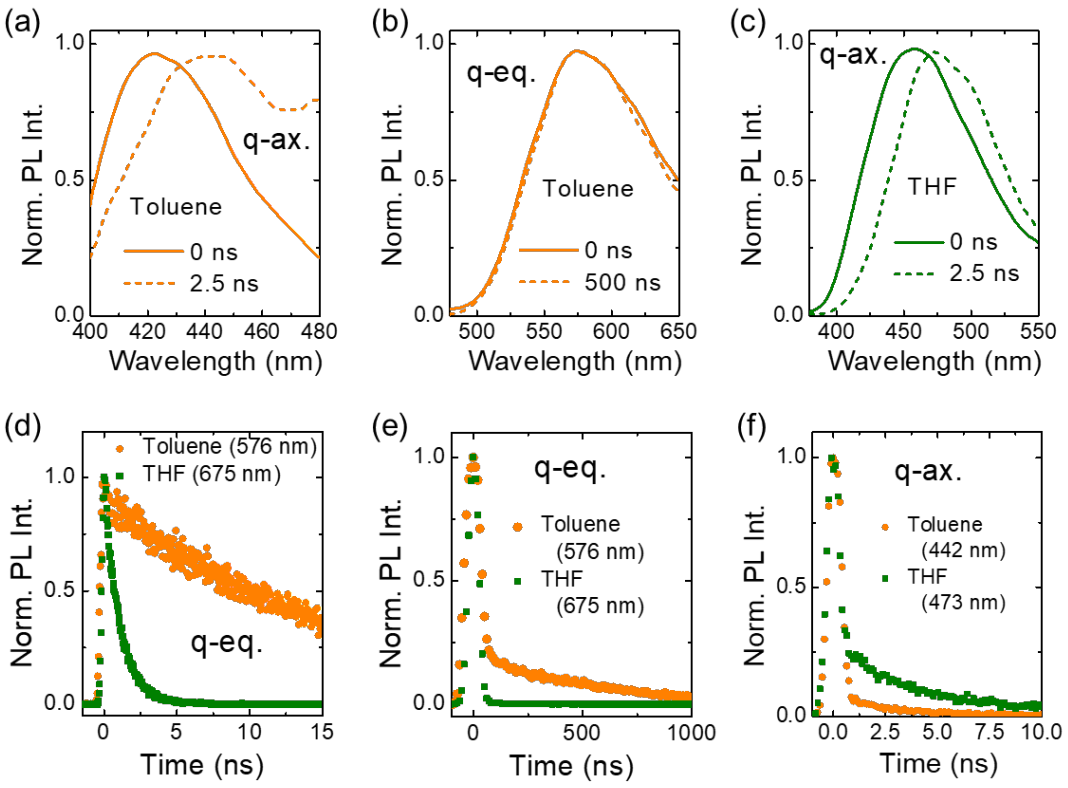

Figure 4. (a-c) Normalized TR-PL spectra of prompt (dashed lines) and delayed (solid lines) components of the q-ax. band in toluene (a), the q-eq. band in toluene (b), and the q-ax. band in THF (c). (d-f) Time profiles of TR-PL spectra of the q-eq. band up to 15 ns (d) and 1000 ns (d) and those of the q-ax. band up to 10 ns (f) in toluene (orange dots) and in THF (green dots). The excitation wavelength was 360 nm.

assigned to TADF because the peak position is different from the shorter lifetime. One rational explanation of this result is that a relaxation from a higher excited state, S_n, to S_1 occurs in less than 1 ns along with the structural change and consequently the relaxed S_1 emits fluorescence with the longer lifetime. Table 2 summarizes all the estimated values from the TR-PL measurements.

Table 2. Determined emission lifetimes of PTZ-TRZ in toluene and THF solution. $\lambda_{q-ax.}$ and $\lambda_{q-eq.}$ are the peak positions of the emission bands of q-ax. and q-eq, respectively. $\tau_{\mathrm{q-ax.}}$ is the first lifetime componet of the emission of q-ax. $\tau_{\mathrm{q-eq.}}^{\mathrm{promt}}$ and $\tau_{\mathrm{q-eq.}}^{delayed}$ are the first and second lifetime components of the emission of q-eq., respectively.

Solvent	$\lambda_{\mathrm{q-ax.}}$ (nm)	$\tau_{\mathrm{q-ax.}}$ (ns)	$\lambda_{\mathrm{q-eq.}}$ (nm)	$\tau_{\mathrm{q-eq.}}^{\mathrm{promt}}$ (ns)	$\tau_{\mathrm{q-eq.}}^{delayed}$ (ns)
Toluene	442	3.6 ± 0.3	576	16 ± 0.1	544 ± 12
THF	473	5.0 ± 0.2	675	0.97 ± 0.01	-

To obtain further information on the dynamics, we measured TA spectra in toluene and in THF shown in Figures 5a and 5b, respectively. A common feature of the TA spectra between the two solvents is that a significant spectral change is observed up to 20 ps and no spectral change is observed after 20 ps. Figures 5c and 5d compare the normalized TA spectra at 100 ps and 1000 ps in toluene and in THF, respectively. To clarify this situation, we compared the temporal profiles ranging from -1.0 ps to 30 ps at longer wavelengths (700 nm for toluene solution, 725 nm for THF solution) and at shorter wavelengths (600 nm for toluene solution and 621 nm for THF solution) shown in Figures 5e and 5f, respectively. At the longer wavelengths, both the profiles are quickly increased less than 1 ps followed by a gradual increase over 20 ps. On the other hand, at the shorter wavelengths, both the profiles are quickly increased less than 1 ps followed by a gradual decrease over 20 ps. Considering that q-ax. partially undergoes a structural change into q-eq. as shown in Figure 1c, both the gradual increase and decrease are assigned to the structural change from q-ax. to q-eq. in the excited states. By the least squares fit using exponential functions, the time constants of structural changes are determined to be 8.0 ± 0.75 ps in toluene and 6.6 ± 0.98 ps in THF. These values are consistent with the time constant for the structural change of ~1.8 ps in the hexane solution reported in the literature [15], considering that the difference in the observed signal between PL and TA.

The temporal profiles at the longer wavelength region in the nanosecond range are shown in Figure 5g. By the least squares fit using exponential functions, the time constants of signal decay were determined to be 15 ± 2.5 ns in toluene and <1 ns in THF. Because these values are close to those of the prompt fluorescence of q-eq. in each solvent, 16 ± 0.1ns in toluene and 0.97 ± 0.01 ns in THF, all the TA spectra after 20 ps are assigned to the transient absorption from S_1 in q-eq. These assignments indicate that only up to 20 ps a weak TA signal from q-ax. is overlaid on a major TA signal from q-eq.

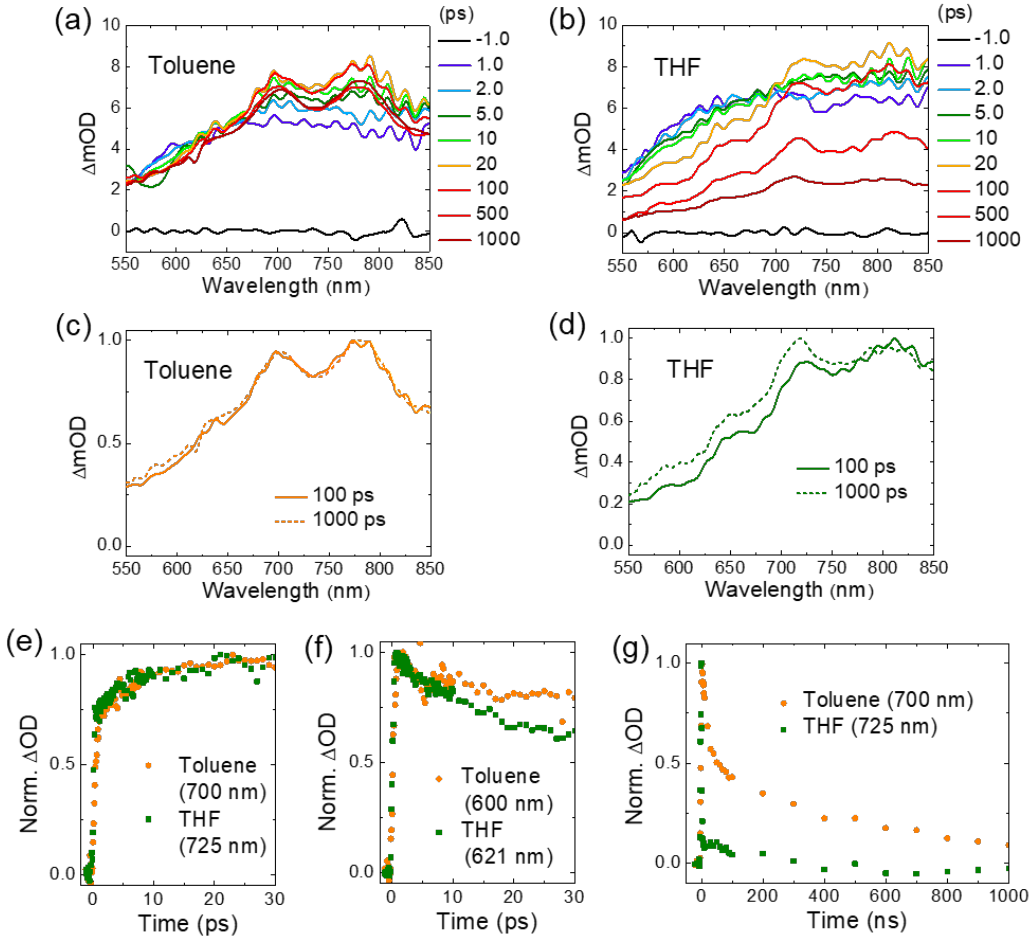

Figure 5. (a, b) Temporal evolutions of TA spectra in toluene (a) and in THF (b). (c, d) Comparison of TA spectra at 100 ps (solid line) and 1000 ps (dotted line) in toluene (c) and THF (d). (e, f) Time profiles in the range of > 690 nm up to 100 ps (c) and up to 1000 ps (d). Orange and green dots represent the data in toluene and THF, respectively. (g) Time profiles in the range of > 690 nm up to 1000 ps. The excitation wavelength was 360 nm for picosecond measurements and 355 nm for nanosecond measurements.

Our proposed model based on these results is shown in Figure 6. In both the solvents, UV irradiation excites both q-ax. and q-eq. to their high excited states (S_n). In toluene, which has the low permittivity solvent (ε=2.38), there are three relaxation processes from S_n in q-ax.: fluorescence with 422 nm, structural change into q-eq with 8.0 ± 0.8 ps lifetime, and internal conversion to S_1. The fluorescence wavelength and lifetime from S_1 are 442 nm and 3.6 ± 0.3 ns, respectively. In q-eq., relaxation from S_n to S_1 occurs quickly in less than 1 ps and also S_1 is generated by the structural change from q-ax. The fluorescence wavelength and lifetime from S_1 are 576 nm and 16 ± 0.1 ns, respectively. Furthermore, the intersystem crossing (ISC) to T_1 followed by the thermal RISC from T_1 occurs and delayed fluorescence is observed with a 544 ± 12 nm lifetime. In THF, which has the high

permittivity (ε = 7.58), the same three processes occur in q-ax. The fluorescence wavelength and lifetime from S_1 are similar to those in toluene, 473 nm and 5.0 ± 0.7 ns, respectively. In contrast, the processes in q-eq. are different from those in toluene. The fluorescence wavelength from S_1 is longer, ~675 nm, and its lifetime is shorter, 0.97 ± 0.01 ns, and no delayed fluorescence is observed. This is presumably because the reduced energy of S_1 in high permittivity solvent accelerates non-radiative relaxation directly to S_0 following the energy gap law.

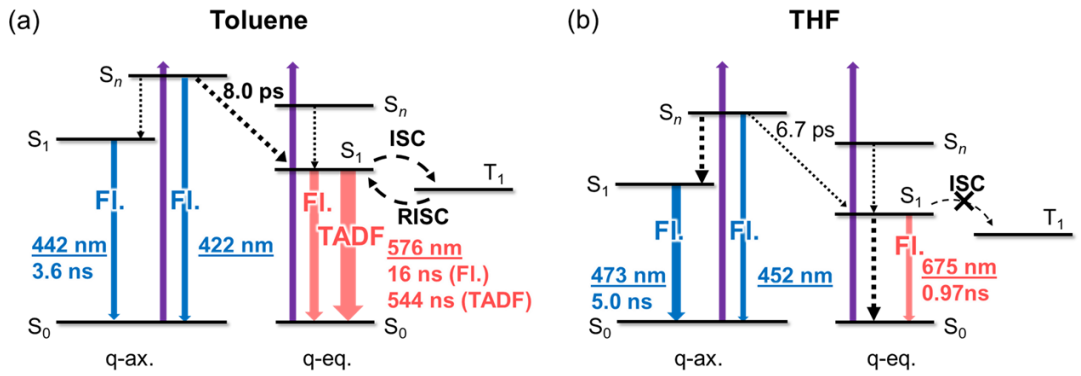

Figure 6. Energy diagram and emission processes in PTZ-TRZ in toluene (a) and in THF (b) after excitation with a 360 nm light.

Conclusion

We investigated the solvent effects on the CT excited states in the quasi-axial (q-ax.) and quasi-equatorial (q-eq.) conformers of PTZ-TRZ using steady-state PL, time-resolved PL, and TA spectroscopies. We determined the dipole moments in the CT excited states from the solvent permittivity dependence of steady-state PL spectra and the Mataga-Lippert equations to be 20.8 D and 23.2 D, respectively. The similarity of these dipole moments was consistent with the quantum chemical calculations. The TR-PL spectra of the q-eq. band showed that the fluorescence wavelength is shorter and the lifetime is longer in toluene (ε = 2.38) than those in THF (ε = 7.58). Moreover, TADF is observed only in toluene. This result is reasonably explained by the model that the stabilization of the S_1 CT state in the higher permittivity solvent, THF, accelerates the non-radiative decay rate and suppresses the ISC to T_1. On the other hand, the TR-PL spectra of the q-ax. band showed similar temporal behavior in both the solvents: the emission band is red-shifted at the longer delay times and there are two distinct lifetime components: less than 1 ns and a few nanoseconds. Judging from the spectral shift and the lifetimes, the states with shorter and longer lifetimes are probably assigned to the highly excited state, S_n, and the lowest singlet state, S_1, respectively. The TA spectra showed a quick spectral change up to 20 ps and no change after 20 ps both in toluene and in THF. This quick spectral change is attributed to the relaxation to S_1 and the structural change from e-ax. to e-eq. in the

highly excited state. Because the time profiles in the nanosecond range are almost the same as those of TR-PL of the q-eq. band, no TA from S_1 in q-ax. is observed probably due to its transition probability. From these results, we elucidated the entire dynamics in the CT states in the two conformers in PTZ-TRZ. The complicated but unique dynamics in CT excited states in a molecule having two conformers would open the way to a new type of photofunctional materials.

Acknowledgements

This work was partially supported by JSPS KAKENHI Grant Numbers JP17H06375, JP20J21226 and JP20H05106 and by JST, the establishment of university fellowships towards the creation of science technology innovation, Grant Number JPMJFS2132. The calculations were carried out using the computer resource by Research Institute for Information Technology, Kyushu University.

References

[1] H. Lu, Y. Zheng, X. Zhao, L. Wang, S. Ma, X. Han, B. Xu, W. Tian, H. Gao, Highly Efficient Far Red/Near-Infrared Solid Fluorophores: Aggregation-Induced Emission, Intramolecular Charge Transfer, Twisted Molecular Conformation, and Bioimaging Applications, Angew. Chemie - Int. Ed. 55 (2016) 155–159. https://doi.org/10.1002/anie.201507031.

[2] W. Chen, S. Xu, J.J. Day, D. Wang, M. Xian, A General Strategy for Development of Near-Infrared Fluorescent Probes for Bioimaging, Angew. Chemie - Int. Ed. 56 (2017) 16611–16615. https://doi.org/10.1002/anie.201710688.

[3] Z.E. Ooi, T.L. Tam, R.Y.C. Shin, Z.K. Chen, T. Kietzke, A. Sellinger, M. Baumgarten, K. Mullen, J.C. DeMello, Solution processable bulk-heterojunction solar cells using a small molecule acceptor, J. Mater. Chem. 18 (2008) 4619–4622. https://doi.org/10.1039/b813786m.

[4] Y. Liang, Z. Xu, J. Xia, S.T. Tsai, Y. Wu, G. Li, C. Ray, L. Yu, For the bright future-bulk heterojunction polymer solar cells with power conversion efficiency of 7.4%, Adv. Mater. 22 (2010) 135–138. https://doi.org/10.1002/adma.200903528.

[5] W.Z. Yuan, Y. Gong, S. Chen, X.Y. Shen, J.W.Y. Lam, P. Lu, Y. Lu, Z. Wang, R. Hu, N. Xie, H.S. Kwok, Y. Zhang, J.Z. Sun, B.Z. Tang, Efficient solid emitters with aggregation-induced emission and intramolecular charge transfer characteristics: Molecular design, synthesis, photophysical behaviors, and OLED application, Chem. Mater. 24 (2012) 1518–1528. https://doi.org/10.1021/cm300416y.

[6] R. Furue, T. Nishimoto, I.S. Park, J. Lee, T. Yasuda, Aggregation-Induced Delayed Fluorescence Based on Donor/Acceptor-Tethered Janus Carborane Triads: Unique Photophysical Properties of Nondoped OLEDs, Angew. Chemie - Int. Ed. 55 (2016) 7171–7175. https://doi.org/10.1002/anie.201603232.

[7] E. Ravindran, N. Somanathan, Efficient and thermally stable non-doped red OLEDs based on a "bird-like" donor-acceptor fluorophore with aggregation induced emission enhancement and intramolecular charge transfer, J. Mater. Chem. C. 5 (2017) 7436–7440. https://doi.org/10.1039/c7tc02253k.

[8] V.M. Korshunov, T.N. Chmovzh, I.S. Golovanov, E.A. Knyazeva, L. V. Mikhalchenko, R.S. Saifutyarov, I.C. Avetisov, J.D. Woollins, I. V. Taydakov, O.A. Rakitin, Candle light-style OLEDs with benzochalcogenadiazoles cores, Dye. Pigment. 185 (2021) 108917. https://doi.org/10.1016/j.dyepig.2020.108917.

[9] Y. Gong, X. Guo, S. Wang, H. Su, A. Xia, Q. He, F. Bai, Photophysical properties of photoactive molecules with conjugated push-pull structures, J. Phys. Chem. A. 111 (2007) 5806–5812. https://doi.org/10.1021/jp0705323.

[10] J. Hu, Y. Li, H. Zhu, S. Qiu, G. He, X. Zhu, A. Xia, Photophysical Properties of Intramolecular Charge Transfer in a Tribranched Donor-π-Acceptor Chromophore, ChemPhysChem. 16 (2015) 2357–2365. https://doi.org/10.1002/cphc.201500290.

[11] A. Endo, K. Sato, K. Yoshimura, T. Kai, A. Kawada, H. Miyazaki, C. Adachi, Efficient up-conversion of triplet excitons into a singlet state and its application for organic light emitting diodes, Appl. Phys. Lett. 98 (2011) 10–13. https://doi.org/10.1063/1.3558906.

[12] H. Uoyama, K. Goushi, K. Shizu, H. Nomura, C. Adachi, Highly efficient organic light-emitting diodes from delayed fluorescence, Nature. 492 (2012) 234–238. https://doi.org/10.1038/nature11687.

[13] H. Tanaka, K. Shizu, H. Miyazaki, C. Adachi, Efficient green thermally activated delayed fluorescence (TADF) from a phenoxazine–triphenyltriazine (PXZ–TRZ) derivative, Chem. Commun. 48 (2012) 11392–11394. https://doi.org/10.1039/c2cc36237f.

[14] H. Tanaka, K. Shizu, H. Nakanotani, C. Adachi, Dual intramolecular charge-transfer fluorescence derived from a phenothiazine-triphenyltriazine derivative, J. Phys. Chem. C. 118 (2014) 15985–15994. https://doi.org/10.1021/jp501017f.

[15] D.G. Chen, T.C. Lin, Y.A. Chen, Y.H. Chen, T.C. Lin, Y.T. Chen, P.T. Chou, Revisiting Dual Intramolecular Charge-Transfer Fluorescence of Phenothiazine-triphenyltriazine Derivatives, J. Phys. Chem. C. 122 (2018) 12215–12221. https://doi.org/10.1021/acs.jpcc.8b04395.

[16] Y. Wang, K.B. Eisenthal, Picosecond dynamics of twisted internal charge transfer phenomena. the role of the solvent, J. Chem. Phys. 77 (1982) 6076–6082. https://doi.org/10.1063/1.443851.

[17] J. Dey, I.M. Warner, Dual fluorescence of 9-(N,N-dimethylamino)anthracene: Effect of solvent polarity and viscosity, J. Phys. Chem. A. 101 (1997) 4872–4878. https://doi.org/10.1021/jp9638696.

[18] A.A.M. Prabhu, R.K. Sankaranarayanan, G. Venkatesh, N. Rajendiran, Dual fluorescence of fast blue RR and fast violet B: Effects of solvents and cyclodextrin complexation, J. Phys. Chem. B.

116 (2012) 9061–9074. https://doi.org/10.1021/jp302162g.

[19] X. Li, G. Baryshnikov, C. Deng, X. Bao, B. Wu, Y. Zhou, H. Ågren, L. Zhu, A three-dimensional ratiometric sensing strategy on unimolecular fluorescence–thermally activated delayed fluorescence dual emission, Nat. Commun. 10 (2019) 1–9. https://doi.org/10.1038/s41467-019-08684-2.

[20] M. Saigo, Y. Shimoda, T. Ehara, T. Ryu, K. Miyata, K. Onda, Characterization of Excited States in a Multiple-Resonance-Type Thermally Activated Delayed Fluorescence Molecule Using Time-Resolved Infrared Spectroscopy, Bull. Chem. Soc. Jpn. 95 (2022) 381–388. https://doi.org/10.1246/bcsj.20210403.

[21] M. Uji, N. Harada, N. Kimizuka, M. Saigo, K. Miyata, K. Onda, N. Yanai, Heavy metal-free visible-to-UV photon upconversion with over 20% efficiency sensitized by a ketocoumarin derivative, J. Mater. Chem. C. 10 (2022) 4558–4562. https://doi.org/10.1039/d1tc05526g.

[22] L. Cui, H. Shinjo, T. Ichiki, K. Deyama, T. Harada, Chromophores : Achieving Multicolor and Circularly Polarized, 0395 (2022). https://doi.org/10.1002/ange.202204358.

[23] M.J. Frisch, G.W. Trucks, H.B. Schlegel, G.E. Scuseria, M.A. Robb, J.R. Cheeseman, G. Scalmani, V. Barone, G.A. Petersson, H. Nakatsuji, X. Li, M. Caricato, A. V. Marenich, J. Bloino, B.G. Janesko, R. Gomperts, B. Mennucci, H.P. Hratchian, J. V. Ortiz, A.F. Izmaylov, J.L. Sonnenberg, D. Williams-Young, F. Ding, F. Lipparini, F. Egidi, J. Goings, B. Peng, A. Petrone, T. Henderson, D. Ranasinghe, V.G. Zakrzewski, J. Gao, N. Rega, G. Zheng, W. Liang, M. Hada, M. Ehara, K. Toyota, R. Fukuda, J. Hasegawa, M. Ishida, T. Nakajima, Y. Honda, O. Kitao, H. Nakai, T. Vreven, K. Throssell, J. Montgomery, J. A., J.E. Peralta, F. Ogliaro, M.J. Bearpark, J.J. Heyd, E.N. Brothers, K.N. Kudin, V.N. Staroverov, T.A. Keith, R. Kobayashi, J. Normand, K. Raghavachari, A.P. Rendell, J.C. Burant, S.S. Iyengar, J. Tomasi, M. Cossi, J.M. Millam, M. Klene, C. Adamo, R. Cammi, J.W. Ochterski, R.L. Martin, K. Morokuma, O. Farkas, J.B. Foresman, D.J. Fox, Gaussian 16, Revision A.03, (2016).

[24] E. Lippert, Dipolmoment und Elektronenstruktur von angeregten Molekülen, Zeitschrift Fur Naturforsch. - Sect. A J. Phys. Sci. 10 (1955) 541–545. https://doi.org/10.1515/zna-1955-0707.

[25] N. Mataga, Y. Kaifu, M. Koizumi, Solvent Effects upon Fluorescence Spectra and the Dipolemoments Excited Molecules * (Received October of By Noboru M ATAGA , Yozo KAIFU and Masao Kolzumi, Bull. Chem. Soc. Jpn. 29 (1956) 465–470.

[26] N. Mataga, Solvent Effects on the Absorption and Fluorescence Spectra of Naphthylamines and Isomeric Aminobenzoic Acids, Bull. Chem. Soc. Jpn. 36 (1963) 654–662. https://doi.org/10.1246/bcsj.36.654.

[27] G. V. Loukova, V.P. Vasiliev, A.A. Milov, V.A. Smirnov, V.I. Minkin, Unraveling electronic properties of an organometallic solute: Lippert-Mataga and quantum-chemical extensive study, J. Photochem. Photobiol. A Chem. 327 (2016) 6–14.

https://doi.org/10.1016/j.jphotochem.2016.04.023.

[28] A. Jouyban, S. Soltanpour, H.K. Chan, A simple relationship between dielectric constant of mixed solvents with solvent composition and temperature, Int. J. Pharm. 269 (2004) 353–360. https://doi.org/10.1016/j.ijpharm.2003.09.010.

[29] W. Heller, Refractive Index Mixture, J. Phys. Chem.. 69 (1965) 1123–1129.

[30] R.L. Martin, Natural transition orbitals, J. Chem. Phys. 118 (2003) 4775–4777. https://doi.org/10.1063/1.1558471.

[31] R. Englman, J. Jortner, The energy gap law for radiationless transitions in large molecules, 8976 (2006). https://doi.org/10.1080/00268977000100171.